

Pre-survey Planning for Microseismic Monitoring Projects

Brad Artman, Ben Witten, and Brad Birkelo*, Spectraseis, Denver, Colorado

brad.birkelo@spectraseis.com

Summary

Each fracture stimulation program has unique aspects that make a one-size-fits-all approach to microseismic monitoring bound to fail. Appropriate design and matching of equipment to the task is essential to delivering high quality information to improve stimulation performance. This paper discusses both the equipment and modeling required to acquire microseismic data that can be most effectively used for hydraulic fracture monitoring. There is no single acquisition geometry that fits all projects. Model examples for both borehole and surface measurements will be presented to demonstrate the advantages and limitations of each. Field data will also be presented, demonstrating the importance of acquisition equipment and survey design.

Introduction

As unconventional resource activities boom, the need to understand the effectiveness of drilling and stimulation programs has led to increased use of microseismic data for well completion evaluation and to define the ideal parameters for future well completions.

Fracture stimulation monitoring is still a relatively new and immature practice within geophysics, with abundant opportunities for smarter data acquisition, processing, and interpretation. This may seem odd given that the foundations of this emerging field rest on decades-old seismological theory and practice (Aki and Richards, 2002). However, with the exploration and development community focused intensely on reflection seismic data in recent decades, some of these basic principles are being rediscovered.

Moreover, as is often the case with new technology applications, the specific questions an operator needs to answer through the acquisition and analysis of microseismic data are not often fully considered beforehand. As a result, limitations of the monitoring survey design may be revealed only after the fact.

In this paper we present intuitive figures created with petrophysical properties and target depths appropriate for the North American resource plays. We show that the radiation of energy from expected seismic emissions illustrates the importance of planning the acquisition geometry, and that weak seismic emissions can be recorded successfully with a newly-available family of highly sensitive, three-component arrays purpose-built for stimulation monitoring.

Set Objectives

The first step an operator should take in planning a microseismic survey is to pose a series of questions for which they need answers. Questions about well and frac stage spacing will likely come to mind first, as these are two important planning areas which contribute profoundly to the economics of resource plays. But there are other challenges and every well is, to some extent, in a unique geologic setting and influenced by the dynamics of historic production and the stimulation program as a whole. These objectives can be severely compromised without the right data acquisition. Thus, after establishing the goals of a proposed survey within an integrated asset team, the geophysicist must then plan and execute the survey to extract the necessary information.

Survey Modeling

Like any complex measurement, success hinges on appropriate planning and modeling before acquisition to ensure that we actually collect the data we need for analysis. The good news is that this modeling and analysis is one of the strongest disciplines in seismology, with accumulated expertise from a century of earthquake studies. Like earthquakes, microseisms are most often small double-couple faults with isotropic and compensated linear vector dipole components (Baig and Urbanic, 2010).

Figure 1 shows the radiation pattern of P-wave energy from a (double-couple) fault. Figure 2 shows the sum of Sv and Sh amplitudes. The horizontal plane shows the distribution of energy incident on the surface, while the sphere below shows the relevant information for planning a borehole deployment. Note that the color bar limits for Figure 1 are +/- 1/8 of the scale on the S-wave energy plot in Figure 2. The vertical fault plane is assumed to strike E-W, indicated by the transparent planes in both. We will assume a horizontal well is drilled perpendicular to the fault plane, through the hypocenter (red dot).

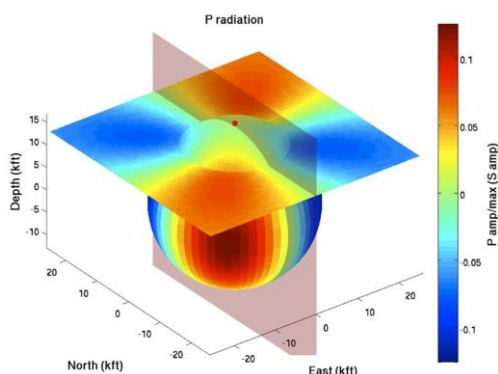


Figure 1: P-wave radiation pattern for a microseismic faulting event. The green colors show two nodal planes where no P energy is recorded. Maximum P energy is 45deg from the transparent fault plane. Color scale range is 1/8th of that in Figure 2.

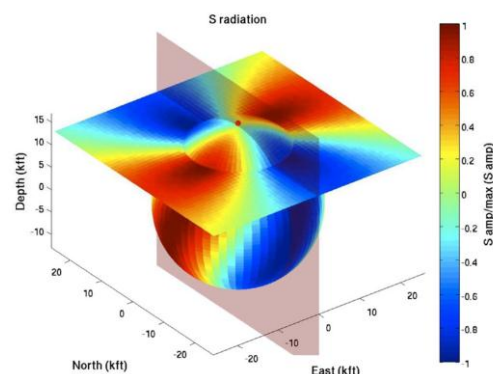


Figure 2: S-wave radiation pattern for a microseismic faulting event. The green colors show two nodal planes where no S energy is recorded. Maximum S energy is within and perpendicular to the transparent fault plane.

Both figures show that there is no energy, P nor S, radiated directly to the surface above the event. Figure 1 shows that a line of geophones on the surface above the horizontal should also record no P arrival. The maximum P amplitudes are 45 deg from the well axis, at a surface offset from the source equal to the depth of the source for this constant velocity example. In a medium where velocity increases with depth, the surface maximum will be closer to the hypocenter due to ray bending. Conversely, in Figure 2, we see that the maximum azimuths for S energy are exactly in the orthogonal coordinate system defined by the well and the fault plane, and S energy is zero where the P is a maximum.

The first priority is usually event location. An array's ability to localize a source within the aperture of the array is trivial, while the distance away from the array is difficult. So, as a general statement, we should expect excellent precision for x,y coordinates from a surface array, while a vertical array should excel at depth resolution. If map coordinates are most important, then an areal array is the obvious choice. If depth accuracy is of paramount importance, deploying a borehole array across and as close as possible to the stimulated interval is the best possible option. However, most borehole arrays have limited aperture, and often don't record the minimum travel path (the top of the hyperbola) when they do not span the reservoir interval.

Algorithms for processing data from both surface and borehole deployments have strengths and weakness that are beyond the scope of this paper. However we will note that the errors inherent in areal geometries are roughly static for all events, while for linear arrays, they increase substantially with

distance. A curious counterpoint arises when we assume a monitor well offset from, but still within, the length of the producer. The minimum distance to the monitor well from a seismic event will be from the stage where the expected fracture planes include the monitor well. Therefore P arrivals are likely to be very weak or not recorded. So even though we know something happened by recording a booming S arrival, calculating locations with only an S event (though theoretically possible) is difficult with a single borehole array in this case. Large aperture arrays of surface or borehole sensors do allow location by acoustic approximations using the S arrivals.

To get both P and S arrivals, the optimal location for a vertical monitor array is therefore halfway between the maximum and minimum of any mode. In this example, the first of 8 best azimuths around the compass is about 25 deg from North, or when the monitor well is located in the back-azimuth from the perforations: $180 \text{ deg} + 25 \text{ deg} = 205 \text{ deg}$.

Data Acquisition Equipment

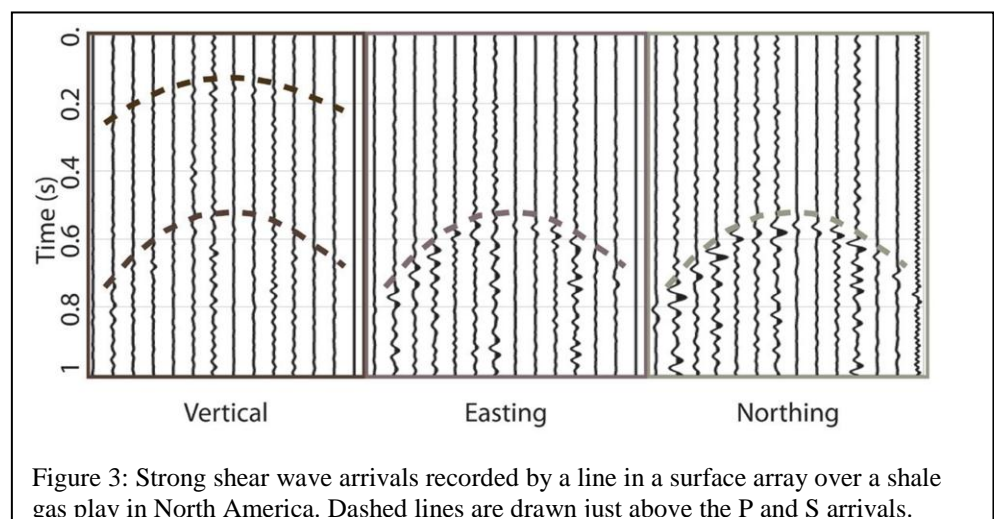
Low-noise, high-sensitivity instruments are essential for capturing relatively weak microseismic energy in most settings, even when using a costly fit-for-purpose observation well.

The standard, general expressions for the radiation of seismic energy from a faulting event are well known and given, for example, in Aki and Richards (2002). Because S-wave velocity is usually about half the P-wave velocity, the Sv and Sh mode amplitudes from a faulting event are 8 times greater than P events. Therefore, considering both S modes together, a microseismic event generates 16 times more shear than compression energy.

Since most of the energy radiated from the source travels as S waves, our first conclusion is that the survey design and processing scheme must properly handle S waves. While using 3C geophones is common practice in downhole applications today, it is unfortunately still common to find surface deployments, and even permanently installed near-surface arrays, constituted only of vertical phones. Microseismic analysis is fundamentally different from familiar reflection surveys, where P-only, vertical component, acoustic approximations have performed so well historically.

Figure 3 is a real event data example showing the dominance of S-wave energy on the horizontal components. Not only does 3C data enable a more complete description of the fractured reservoir, 1C data simply ignores a huge amount of important energy from the fractures.

The size of events that can be measured with a given geometry is also an important parameter. The amplitude spectrum of a faulting source has been empirically confirmed to follow a model (Brune, 1970) that is a function of the size of the event. With a local velocity model and an estimate of attenuation, we can quickly generate estimates of event



distance of an array from the event. In the models that follow we assume the event is 2,000 ft away, a constant Q of 150, a Vp/Vs ratio of 2 and Vp=9,600 ft/s.

Figure 4 shows modeled amplitude spectra of nominal events compared to average background noise levels and two geophone sensitivity curves, plotting seismic energy as a function of frequency. The series of red lines are fracture spectra with calculated moment magnitudes of -3.5 to -1.0 events in steps of 0.5. The gray lines are the upper and lower bounds of seismic background noise continuously present in the Earth's crust (Peterson, 1993). The blue dashed line is the sensitivity threshold, or noise floor, of a generic 15 Hz geophone often used for surface and downhole microseismic monitoring.

The green dashed line is the same measure for a modern amplified geophone receiver. The receivers achieve a 50x sensitivity increase, enabling the recording of half-magnitude weaker events from the same distance (or the same magnitude from much further away). The sensors record events that are stronger than background noise, rather than being limited by instrument self-noise. In all cases, a microseismic event will have a higher signal-to-noise ratio and be better characterized with the more sensitive equipment, assuming that the borehole noise is less than the instrument noise floor of the 15-Hz geophone.

Conclusions

As microseismic service providers gain experience and perfect their craft, more insightful products are being delivered that answer

important questions about the effectiveness of the stimulation dollars being spent on North American resource plays. Each program has unique aspects that make a one-size-fits-all approach likely to fail.

It is critical to define the objectives of a fracture monitoring program carefully, and then design a program that has the best chance of success. Selecting the acquisition geometry, equipment and processing methods most appropriate for the stimulation will assure delivery of a valuable product.

Microseismic analysis is fundamentally different from familiar reflection surveys, where P-only, vertical component, acoustic approximations have performed so well historically. Acquisition and analysis of these data require that we think and act more like the earthquake seismologists in order to gain the full benefit of this data type.

References

- Aki and Richards, 2002, *Quantitative Seismology*, Second Edition, University Science Books.
 Baig, A., and Urbanic, T., 2010 Microseismic moment tensors: A path to understanding frac growth, *The Leading Edge* 29, 320-324.
 Brune, J., 1970, Tectonic Stress and the Spectra of Seismic Shear Waves from Earthquakes, *JGR* 75(26), 4997—5009.
 Peterson, J., 1993, Observations and modeling of seismic background noise, USGS Open File Report 93-322.

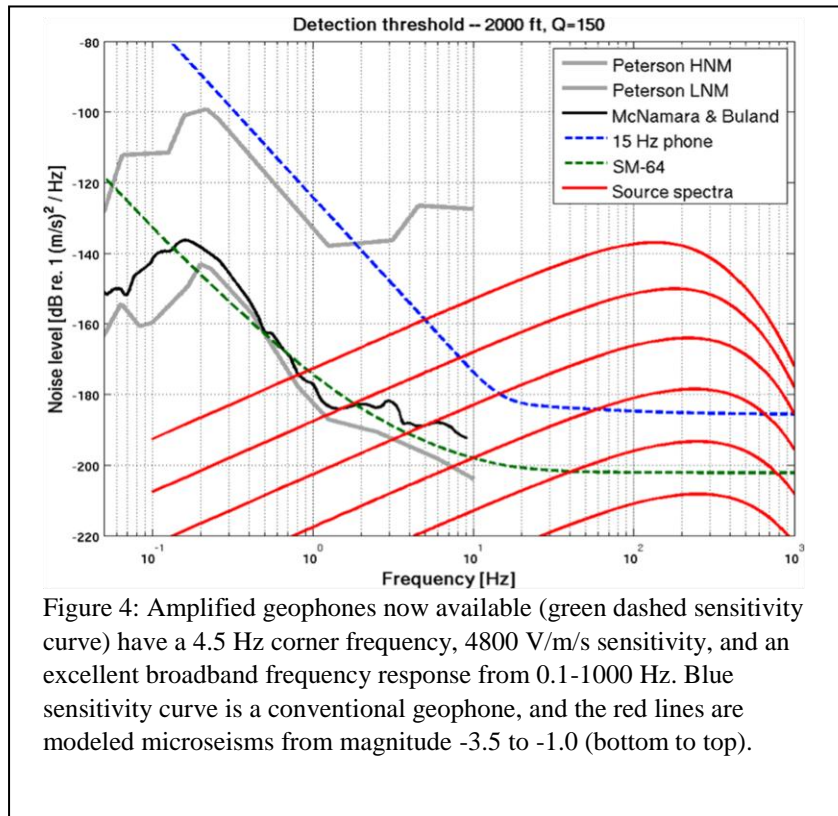


Figure 4: Amplified geophones now available (green dashed sensitivity curve) have a 4.5 Hz corner frequency, 4800 V/m/s sensitivity, and an excellent broadband frequency response from 0.1-1000 Hz. Blue sensitivity curve is a conventional geophone, and the red lines are modeled microseisms from magnitude -3.5 to -1.0 (bottom to top).